Earthquakes and Structures, *Vol. 4, No. 6 (2013) 629-647*
DOI: http://dx.doi.org/10.12989/eas.2013.4.6.629

Protocol for testing of cold-formed steel wall in regions of low-moderate seismicity

Rojit Shahi*[1], Nelson Lam[1], Emad Gad[2] and John Wilson[2]

[1]*Department of Infrastructure Engineering, The University of Melbourne, Parkville, VIC 3010, Australia*
[2]*Faculty of Engineering and Industrial Sciences, Swinburne University of Technology, Hawthorn, VIC 3122, Australia*

(Received July 03, 2012, Revised January 17, 2013, Accepted January 22, 2013)

Abstract. Loading protocols have been developed for quasi-static cyclic testing of structures and components. However, it is uncertain if protocols developed for conditions of intense ground shaking in regions of high seismicity would also be applicable to regions of low-moderate seismicity that are remote from the tectonic plate boundaries. This study presents a methodology for developing a quasi-static cyclic displacement loading protocol for experimental bracing evaluation of cold-formed steel stud shear walls. Simulations presented in the paper were based on conditions of moderate ground shaking (in Australia). The methodologies presented are generic in nature and can be applied to other regions of similar seismicity conditions (which include many parts of China, Korea, India and Malaysia). Numerous response time histories including both linear and nonlinear analyses have been generated for selected earthquake scenarios and site classes. Rain-flow cycle counting method has been used for determining the number of cycles at various ranges of normalized displacement amplitude. It is found that the number of displacement cycles of the loading protocol increases with increasing intensity of ground shaking (associated with a longer return period).

Keywords: loading protocols; low-moderate seismicity; cold-formed steel stud shear walls; number of cycles; normalized displacement amplitude

1. Introduction

In structural design practices, the seismic demand is typically expressed by Standards (or Codes of Practices) in terms of ground motion parameters such as the peak ground acceleration and response spectral accelerations. However, the level of response of the structure and the amount of damage sustained by it in an earthquake can vary significantly even with similar peak ground acceleration values, as much depends on the nature of the ground shaking (Iervolino and Cornell 2005). In reality, the actual demands of an earthquake can only be represented by the time-history of the ground shaking whereas the actual capacity of a structure can be sensitive to its cyclic response behaviour to the applied excitations. In other words, neither ground motion parameters nor elastic analyses of the structure on their own based on a stipulated response spectrum model can be relied upon to predict performance.

*Corresponding author, PhD Candidate, E-mail: r.shahi2@pgrad.unimelb.edu.au

http://www.techno-press.org/?journal=eas&subpage=7 ISSN: 2092-7614 (Print), 2092-7622 (Online)

The subject matter of this paper forms part of the research undertakings which are concerned with the performance assessment of cold-formed structural steel in domestic low-rise buildings in industrialized countries. The interaction between demand and capacity of composite actions of cold-formed steel stud shear walls under cyclic strain reversals in an earthquake can be too complex to analyse and is best evaluated by physical experimentation. Static racking tests on their own with this form of construction would not automatically capture the complex coupling between seismic demand and capacity, nor the cyclic degradation in strength and stiffness. The aseismic design of cold-formed steel stud shear walls would need to take into account relevant dynamic phenomena and cyclic ductility behaviour in the post-elastic range.

An effective program of physical experimentation would need to incorporate representative cyclic reversal characteristics of the design earthquake. The main challenge is in identifying such characteristics for incorporation into the experiments (without having to repeat the tests too many times using different accelerograms) whilst effectively addressing the high variabilities of earthquake ground shaking for given intensity limits. An innovative ground motion selection procedure involving incremental dynamic analyses have been developed in order that pseudo-dynamic, or dynamic (shaking table), testings on the structural specimen would only need be executed for three accelerogram records selected from the procedure (Dhakal *et al.* 2006, 2007, Bradley *et al.* 2008). The complex demand-capacity interactions in dynamic conditions of the design earthquake can be modelled by this combination of analytical and physical simulations.

Dynamic testing of a full scale specimen of a domestic house built of cold-formed steel on the shaker table has been carried out by the authors in a recent investigation (Paton-Cole *et al.* 2011). Dynamic testings of this nature could still be overly costly, and impractical, even if a small number of accelerograms are being used given that the tests have to be repeated for different design configurations. It is much more expedient and appropriate, to employ quasi-static cyclic testings in lieu of dynamic testings to evaluate the seismic performance of this form of construction, and more so in regions of low and moderate seismicity. A quasi-static test is not associated with any particular accelerogram. The number of load reversals is simply pre-determined by a loading protocol which is representative of the seismicity of the area, site conditions and potential response behaviour of the structures concerned. It is the primary objective of this paper to develop such a protocol. Once the hysteretic behaviour of the structural system has been modelled (from results obtained by quasi-static cyclic testing) the potential dynamic behaviour in seismic conditions could be simulated by non-linear time-history analyses.

A loading protocol which defines the number of half-cycles of loading and unloading at different normalized amplitudes of displacement excursion would be required in every quasi-static cyclic test. Some well known loading protocols shown in Fig. 1 have been recommended for the testing of structural and non-structural components (Krawinkler 1996, FEMA 2007), steel structures (ATC-24 1992), wood/masonry structures (Porter 1987), bracing walls in low-rise buildings (Cooney and Collins 1988, King and Lim 1991, Herbert and King 1998). However, it is noted that accelerograms used in the development of these protocols were of a diverse range of conditions and not exclusively based on earthquake scenarios that would impose the most onerous drift demand on low-rise buildings (with natural period in the range 0.1–0.4 sec). The loading protocol of Della *et al.* (2006) was developed for the design of cold-formed steel structures but was intended to be used in areas of high seismic activities, including certain parts of Italy. Thus, the frequency content of the (scaled) accelerograms used in the study were not consistent with that of small-medium magnitude (M5.5 to M7) earthquakes which design in areas of low-moderate seismicity, like Australia, are based upon. The loading protocols so developed in this paper shall

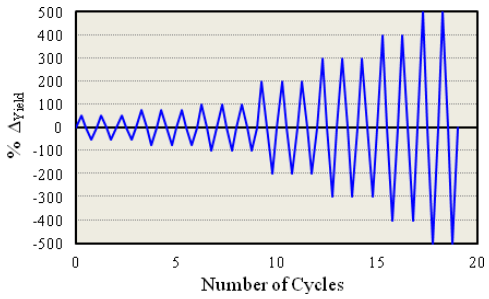

(a) ATC-24 protocol (ATC-24 1992)

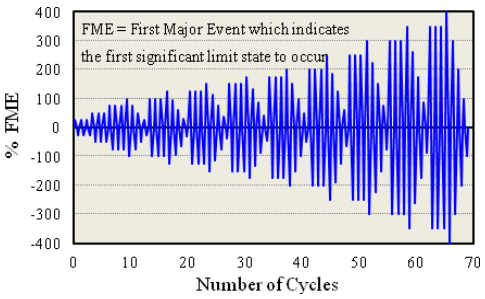

(b) SPD protocol (Porter 1987)

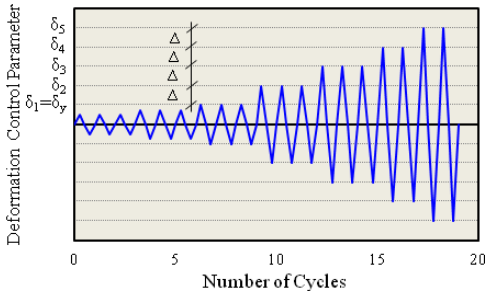

(c) Multiple step test (Krawinkler 1996)

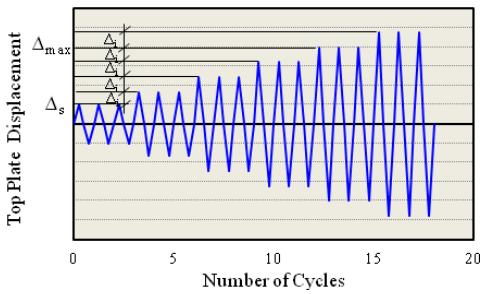

(d) P21 test protocol (Cooney and Collins 1988, King and Lim 1991, Herbert and King 1998)

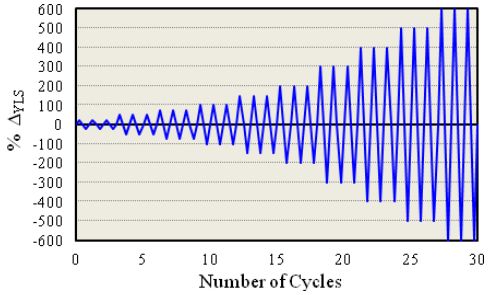

(e) Cyclic test protocol (Della *et al.* 2006)

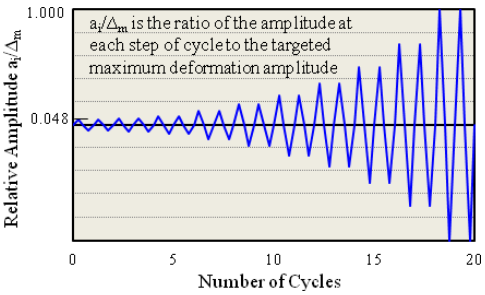

(f) FEMA 461 (FEMA 2007)

Fig. 1 Typical loading protocols for seismic testing

provide realistic representation of the seismic demands in areas of low-moderate seismicity for a return period of 500 years. The same process can be applied for longer return periods if required. A sample simulation has also been performed for the earthquake scenario associated with a return period of 2500 years. Future experimental work in developing design guidelines for lateral bracing elements in domestic buildings built of cold-formed steel will have to conform to these protocols.

This paper presents the development of a model loading protocol that has been derived from earthquake scenarios (combination of magnitude, distance and sub-soil conditions) which feature: (i) frequency contents that would be critical to the design of shear walls built of cold-formed steel studs and (ii) conditions of moderate ground shaking that is assumed for regions away from tectonic plate boundaries, like Australia.

The rest of the paper is structured as follows: (i) Section 2 identifies probable earthquake scenarios that are consistent with a notional peak ground acceleration level of 0.05–0.11 g on rock

as stipulated by the Australian Standard (AS1170.4 2007) for a notional return period of 500 years; (ii) Section 3 provides details of artificial accelerograms that have been generated and verified, for these identified earthquake scenarios on rock sites using the well established methodology of stochastic simulations (Accelerograms for various subsoil conditions have also been simulated accordingly); (iii) Section 4 identifies critical combinations of earthquake scenarios and site classes which impose the highest drift demand on cold-formed steel stud shear walls; and finally (iv) Section 5 develops a model loading protocol based on the use of the *rain-flow cycle counting method* and observations of response time-histories that have been simulated for the identified critical scenarios and site conditions.

2. Probable earthquake scenarios

Most of the world's earthquakes occur on well defined tectonic plate boundaries and are known as interplate earthquakes. Intraplate earthquakes, which are associated with regions of low-moderate seismicity, occur far away from the tectonic plate boundaries. Globally, the majority of earthquakes are interplate earthquakes and less than 10% are intraplate earthquakes. This statistical data reveals that there is paucity of strong motion database in an intraplate region and hence conventional regression analysis cannot be applied. Hence, artificial accelerograms are generated by stochastic simulations of the seismological model. The artificial accelerograms have been generated by the aid of program GENQKE that was developed at the University of Melbourne (Lam 1999, Lam *et al.* 2000).

2.1 Preliminary selection of earthquake scenario for stochastic simulation

The first step of the study was to determine probable earthquake scenarios rather than selecting ground motion records from different sources as in the case of protocols developed earlier (Porter 1987, ATC-24 1992, Krawinkler 1996, Della *et al.* 2006, FEMA 2007). Probable earthquake scenarios refer to the earthquake scenarios which contribute to the desired level of notional peak ground acceleration (seismic hazard) for the region of interest for a notional return period and hence no scaling of ground motion is required. As for example in the case of Australia, the probable earthquake scenarios refer to the earthquake scenarios with a notional peak ground acceleration (or seismic hazard factor; k_PZ) of between 0.05 g and 0.11 g for a return period of 500 years (10% probability of exceedance in a design life of 50 years). Such probable earthquake scenarios can be determined by de-aggregation analyses forming part of the probabilistic seismic

Table 1 Seismic hazard factor (k_PZ) predicted from Gaull's model

Distance\Magnitude	*M*5.5	*M*6	*M*6.5	*M*7
15 km	0.120*	0.202	0.340	0.571
20 km	0.086	0.144	0.242	0.407
30 km	0.053	0.090	0.151	0.253
50 km	0.029	0.049	0.083	0.139
70 km	0.020	0.033*	0.056	0.094
100 km	0.013	0.022	0.037*	0.062
150 km	0.008	0.014	0.023	0.038*

hazard analysis (PSHA) procedure. However, in view of uncertainties in the spatial distribution of potential seismic sources within the Australian continent, it is prudent to adopt the more conservative approach of considering all probable earthquake scenarios of between magnitude 5.5 and 7.0 which could generate the stipulated level of peak ground accelerations. These selected earthquake scenarios expressed in terms of magnitude - distance combinations are considered to be of engineering interests and are appropriate for stable continental regions like Australia where earthquakes of up to magnitude 7 are considered to be plausible. These probable scenarios could be identified by back calculations using ground motion predictive relationships of Gaull *et al.* (1990) as defined by Eqs. 1(a) and 1(b) (from which the seismic hazard map for South-Eastern Australia was developed by PSHA). A uniform distribution of seismic activity is assumed when this approach is used.

$$\text{MMI} = 1.5M - 3.9 \log R + 3.9 \tag{1a}$$

$$2^{\text{MMI}} = 7/5 \text{ PGV (avg. site)} \tag{1b}$$

$$\text{PGV (rock)} = \text{PGV (avg. site)}/\ 1.5 \tag{1c}$$

$$k_P Z = 750/\ \text{PGV (rock)}\ (k_P = 1.0 \text{ for return period of 500 years}) \tag{1d}$$

where, MMI is the Modified Mercalli Intensity scale, M is the moment magnitude of the earthquake; R is the site-source distance in km and PGV is peak ground velocity in mm/s

Eq. 1(a) was derived from Iso-seismal maps of historical earthquakes recorded in South-Eastern Australia (Gaull *et al.* 1990). The MMI-PGV conversion relationship of Eq. 1(b) was based on recommendations by Newmark and Rosenbleuth (1971). More updated conversion relationships have since been developed (Atkinson and Sonely 2000, Atkinson and Kaka 2007, Yaghmaei-Sabegh *et al.* 2011) but discrepancies between these relationships are not significant enough to justify using an expression different to Eq. 1(b) for the purpose of indentifying the probable earthquake scenarios. These predicted values of PGV from the Intensity model of Gaull were based on "Average" site conditions which may be assumed to be about 1.5 times higher than that for "rock" conditions (Lam *et al.* 2003 and 2005). Hence, the predicted values of PGV for "rock" sites were obtained by dividing the results from Eqs. 1(a) and 1(b) by a factor of 1.5 in Eq. 1(c). As explained in the commentary to the Australian Standard (AS1170.4 2007), Eq. 1(d) is for

Table 2 Selection of *M*-*R* combinations for stochastic simulation

Distance\Magnitude	*M*5.5	*M*6	*M*6.5	*i*7
15 km	√	---	---	---
20 km	√	---	---	---
30 km	√	√	---	---
50 km	---	√	√	---
70 km	---	√	√	√
100 km	---	---	√	√
150 km	---	---	---	√

[*] *$k_P Z$ ~ 0.05-0.11 g are also selected which are marked by [*] in* Table 1

Table 3 Simulated notional PGV values (mm/sec) for identified M-R combinations

Distance\Magnitude	*M*5.5	*M*6	*M*6.5	*M*7
15 km	85	---	---	---
20 km	61	---	---	---
30 km	39	74	---	---
50 km	---	40	65	---
70 km	---	31	57	86
100 km	---	---	40	63
150 km	---	---	---	40

Table 4 Simulated seismic hazard factor (k_PZ) for identified *M-R* combinations

Distance\Magnitude	*M*5.5	*M*6	*M*6.5	*M*7
15 km	0.11	---	---	---
20 km	0.08	---	---	---
30 km	0.05	0.10	---	---
50 km	---	0.05	0.09	---
70 km	---	0.04	0.08	0.11
100 km	---	---	0.05	0.08
150 km	---	---	---	0.05

finding values of the notional peak ground acceleration, k_PZ, based on the calculated peak ground velocity values. Results are summarized in Table 1 for a range of earthquake scenarios. Magnitude-distance (*M-R*) combinations that are associated the value of k_PZ within the range of 0.05–0.11 g has been identified with *ticks* in Table 2.

3. Stochastic simulated accelerograms

For every probable earthquake scenarios that are defined by the M-R combinations listed in Table 2, artificial accelerograms were generated by stochastic simulations of the seismological model using program GENQKE. Refer to review paper by Lam *et al.* (2000) for a detailed illustration of the simulation methodology. The seismological model used for simulating intraplate earthquakes comprises the source model of Lam and Chandler (2005), the path attenuation model of Chandler and Lam (2004) and the crustal model of Chandler *et al.* (2005, 2006). Local conditions specific to South-Eastern Australia have been incorporated into the refinement of the seismological model (Lam *et al.* 2006). The simulation model has been verified by comparison of the simulated ground motion parameters with information inferred from intensity data of historical events recorded in Australia (Lam *et al.* 2003, 2005, 2006). Samples of the simulated accelerograms on both rock and soil sites are available for downloading from the website of the *Electronic Journal of Structural Engineering* (Lam *et al.* 2005).

For every probable *M-R* combination (Table 2), an ensemble of artificial accelerograms were simulated and analyzed to obtain their respective response spectra. Notional peak ground velocity

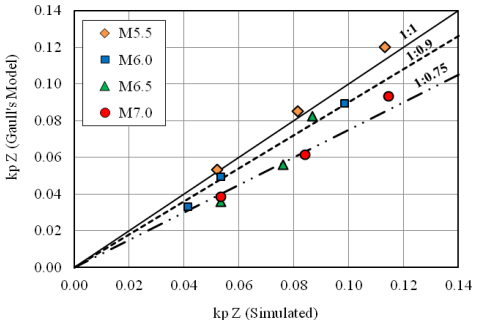

Fig. 2 k_PZ values from simulated accelerograms and Gaull's model

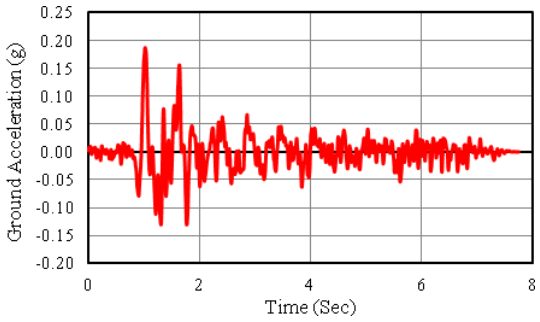

(a) Recorded earthquake
(N. Pam Springs 1986, M~6.0; R~30 km)

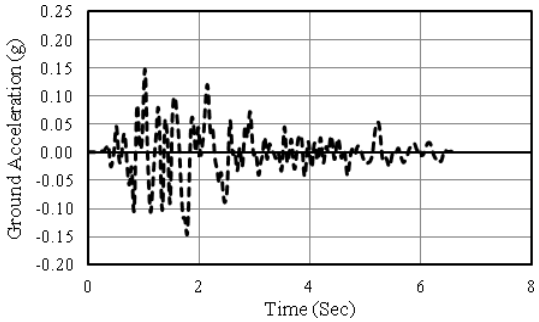

(b) Stochastic simulation (M = 6.0; R = 30 km)

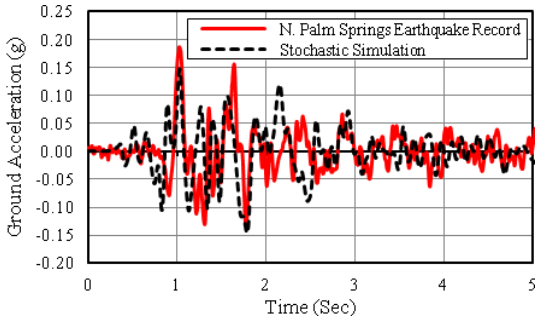

(c) Strong motion records only

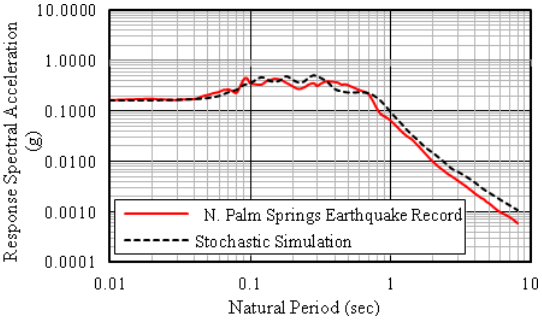

(d) Response spectra

Fig. 3 Comparison between simulated accelerogram and recorded earthquake

(PGV) on "rock" site is defined as the highest ensemble averaged velocity response Spectrum (RSV_{max}) value divided by the factor of 1.8 (as defined by the commentary to the Australian Standard (AS1170.4 2007). Notional PGV values so obtained for the identified *M*-*R* combinations are summarized in Table 3.

Notional peak ground acceleration values (or seismic hazard factor, k_PZ) were then calculated from the simulated PGV values listed in Table 3 (using Eq. 1(d)). Results are shown in Table 4 below for comparison with values calculated from the empirical model of Gaull (1990) as listed in Table 1. The demonstrated consistency between the two sets of values (shown explicitly in the

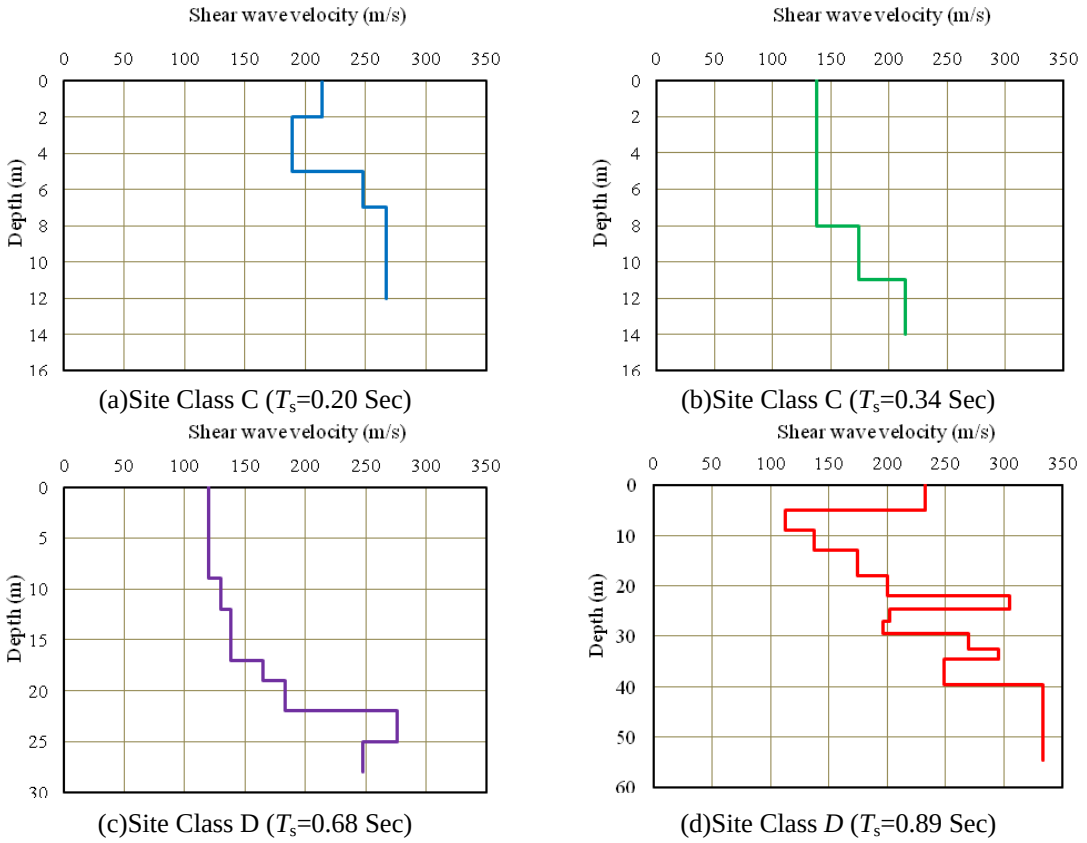

Fig. 4 Example borehole logs and shear wave velocity profiles

correlation plot of Fig. 2) serves to verify the use of the artificial accelerograms for representing the seismic demand on structures.

The stochastic simulated accelerograms have also been compared with recorded accelerograms (PEER ground motion database, PEER 2005) for different M-R combinations on rock and shallow soil sites. One sample comparison between the stochastically generated accelerogram and the recorded earthquake for M = 6.0 and R = 30 km is shown in Fig. 3. It is noted that the duration of earthquake (Figs. 3(a) and 3(b)), the frequency content and the number of strong motion cycles (Fig. 3(c)) of the artificial accelerogram generated from program GENQKE are found to be consistent with the recorded earthquake (North Palm Springs 1986). The acceleration response spectra for the generated and the recorded earthquakes are plotted in Fig. 3(d). The demonstrated consistency between the artificially generated and the recorded accelerograms serves to support the use of GENQKE for generating artificial accelerograms. Further evidences of consistencies between the recorded and seismological data can be found in Lam *et al.* (2001), Balendra *et al.* (2002), Hutchinson *et al.* (2003), Chandler and Lam (2004), Lam and Chandler (2005), Lam *et al.* (2009) and Yagmaei-Sabegh and Lam (2010).

4. Critical combinations of earthquake scenarios and site class

Artificial accelerograms simulated from the seismological model are based on rock conditions. These simulations have been extended to cover for conditions on soil sites by one-dimensional pseudo-nonlinear analyses of soil column models using program SHAKE (Idriss and Sun 1992). Borehole records were analysed to estimate shear wave velocity profiles in the subsoil layers using relationships recommended by Lam and Wilson (1999). A large number of shear wave velocity profiles have been analysed and sorted in accordance with their estimated site natural period. Samples of these profiles and their calculated site natural periods consistent with site class C and D as per AS1170.4 (2007) are shown in Figs. 4(a)–4(d). Site response spectra in different formats calculated from accelerograms simulated on the soil surface are shown in Figs. 5(a)–5(d).

The initial period of cold-formed steel buildings in Australia (with one or two storeys) ranges from 0.1–0.2 sec and can be lengthened as a result of stiffness degradation (to about 2 times its initial natural period value) in severe earthquake conditions. Thus, response of the structure within the natural period range of 0.1–0.4 sec is of interests in this study. Response spectra presented in the displacement format (Fig. 5(c)) or acceleration- displacement format (Fig. 5(d)); provide direct indications of the seismically induced drift demand on structures. Soil amplification factors are shown to be dependent on the site natural period given that there is a trend of increase in value of the site amplification factor with increasing site natural period (site factors in order of 2.0, 2.5, 3.5 and 4.0 for site natural period of 0.20, 0.34, 0.68 and 0.89 sec respectively). Importantly, more onerous displacement demand in the natural period range of 0.1–0.4 sec is shown on the displacement spectra for site class C than site class D. It is revealed in Figs. 5(c) and 5(d) (representing earthquake scenarios of M = 6.5 & R = 50 km) that the displacement demand on structures in this natural period range is less than 10 mm for site class D whereas it is in the order of 15 mm - 25 mm for site class C. However, more onerous displacement demand in the higher period range (*ie* > 0.4 sec) is estimated for site class D than site class C.

Analyses for the displacement demand have been conducted for shear wave velocity profiles of Figs. 4(a) – 4(d) for every probable earthquake scenarios identified in Tables 2-4. It was found that earthquake scenarios: (i) M = 5.5 & R = 15 km, (ii) M = 6.0 & R = 30 km and (iii) M = 6.5 & R = 50 km would generate higher seismic demand on structures with natural period of up to 0.4 sec than other earthquake scenarios considered in this study. Displacement demand on site class C (Figs. 6(a) and 6(b)) is shown to be much higher than that on site Class D (Figs. 6(c) and 6(d)) in this range of natural period. Critical combinations of earthquake scenarios and shear wave velocity profiles (identified by site natural period, T_s) that have been identified by the parametric study are listed in Table 5. Earthquake scenario of M = 7.0 & R = 70 km is not listed because such long distance scenario would only be onerous to the more flexible structures with natural period value higher than 0.4 sec. Displacement demand on very stiff structures (with a natural period of 0.1 sec) is also considered to be not critical in view of the very low (< 5 mm) displacement demand.

5. Cyclic behaviour of critical scenarios and loading protocol recommendation

Artificial accelerograms simulated for the critical combinations of earthquake scenarios and shear wave velocity profiles (Table 5) were subjected to time history analyses for simulating the response behaviour of single-degree-of-freedom (SDOF) systems for 5% damping using standard

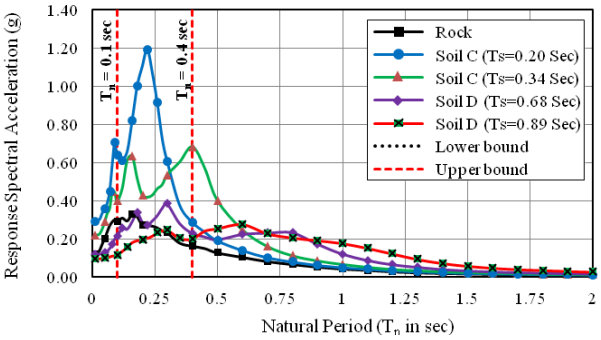

(a) Acceleration response spectra

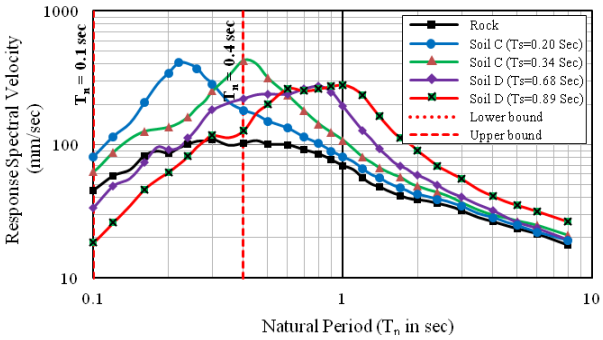

(b) Velocity response spectra

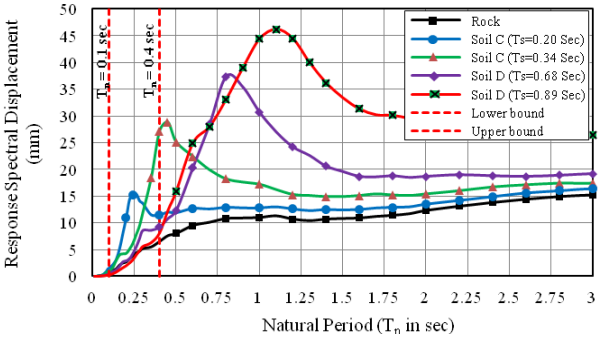

(c) Displacement response spectra

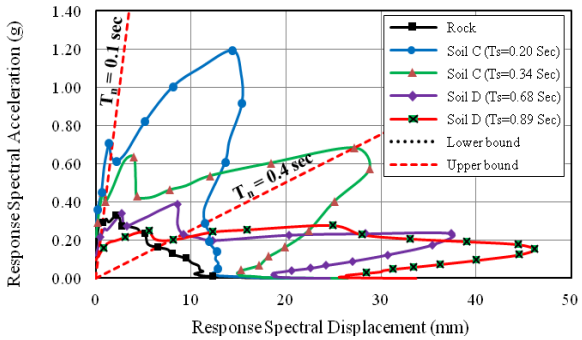

(d) Acceleration-displacement response spectra (ADRS)

Fig. 5 Response spectra simulated on rock and soil sites (M = 6.5 & R = 50 km)

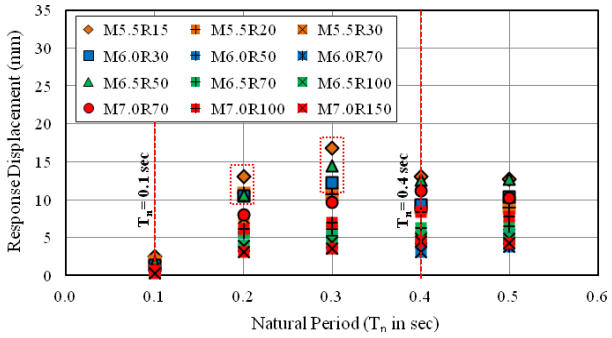

(a) Site Class C (*Ts*=0.20 Sec)

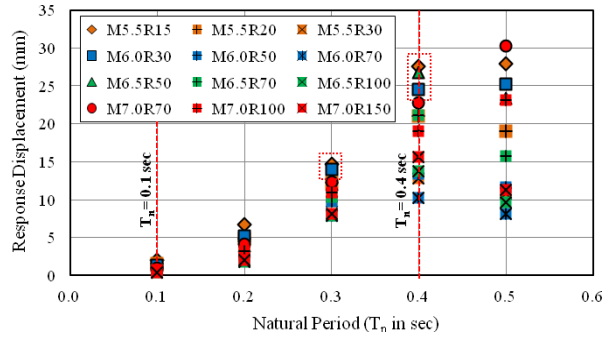

(b) Site Class C (*Ts* = 0.34 Sec)

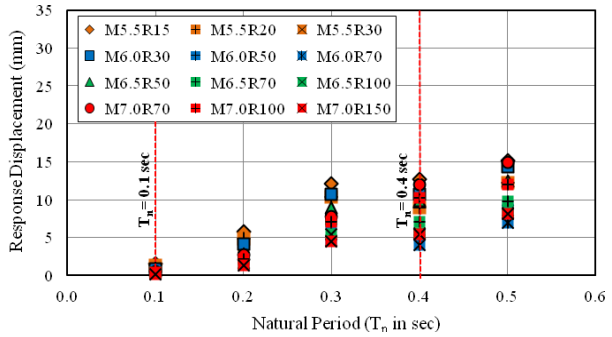

(c) Site Class D (*Ts* = 0.68 Sec)

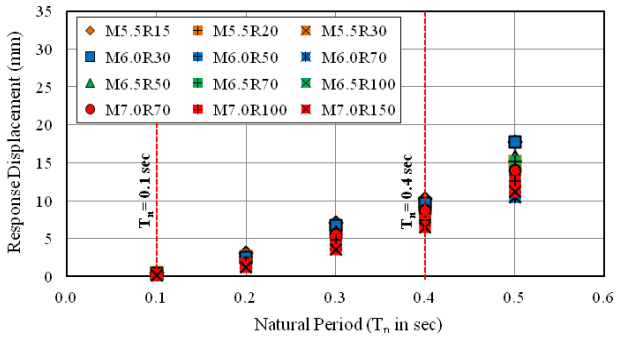

(d) Site Class D (*Ts* = 0.89 Sec)

Fig. 6 Elastic response displacement for various selected earthquake scenarios with different sub-soil conditions

Table 5 Critical combinations of earthquake scenarios

Case	Natural period of structure (T_n in sec)	Site class	Specific earthquake scenario	No. of accelerograms
1	0.2	Site Class C (T_S =0.20 Sec)	*M*5.5*R*15	6
2	0.2	Site Class C (T_S =0.20 Sec)	*M*6.0*R*30	6
3	0.2	Site Class C (T_S =0.20 Sec)	*M*6.5*R*50	6
4	0.3	Site Class C (T_S =0.20 Sec)	*M*5.5*R*15	6
5	0.3	Site Class C (T_S =0.20 Sec)	*M*6.0*R*30	6
6	0.3	Site Class C (T_S =0.20 Sec)	*M*6.5*R*50	6
7	0.3	Site Class C (T_S =0.34 Sec)	*M*5.5*R*15	6
8	0.3	Site Class C (T_S =0.34 Sec)	*M*6.0*R*30	6
9	0.3	Site Class C (T_S =0.34 Sec)	*M*6.5*R*50	6
10	0.4	Site Class C (T_S =0.34 Sec)	*M*5.5*R*15	6
11	0.4	Site Class C (T_S =0.34 Sec)	*M*6.0*R*30	6
12	0.4	Site Class C (T_S =0.34 Sec)	*M*6.5*R*50	6

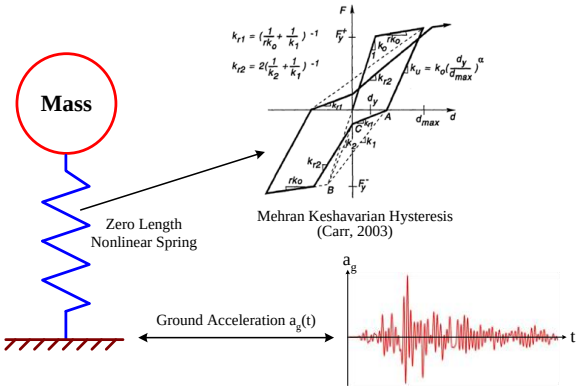

Fig. 7 Hysteretic model employed for non-linear time history analyses

methods presented in Chopra (2007). Computer program Ruoumoko2D (Carr 2003) was used to operate non-linear time-history analyses. Fig. 7 shows the representation of the numerical model by the use of zero length nonlinear spring (pinch hysteresis behaviour) in a lumped mass SDOF system. The mass and stiffness values of the building models have been calibrated in order that their natural period of vibration are in the range 0.2–0.4 sec to emulate the behaviour of one or two storey light framed domestic houses. Strength degradation of the system was defined as a function of the ductility value (μ). Linear degradation from full strength was assumed to commence at ductility value of 4 to residual strength (30% of full strength) at ductility value of 6. Stiffness degradation of the system was controlled by the unloading stiffness parameter (α) which was set at 0.2 in the analyses. The normalized response displacement time histories as obtained from the analyses for one of the considered earthquake scenarios (Case 8 of Table 5) are shown in Fig. 8.

Rain-flow counting method was used to determine the number of cycles for various levels of normalized amplitude of displacement. Fig. 9 shows the cycle counts for every simulation associated with the example earthquake scenario (Case 8 of Table 5) to illustrate inter-event

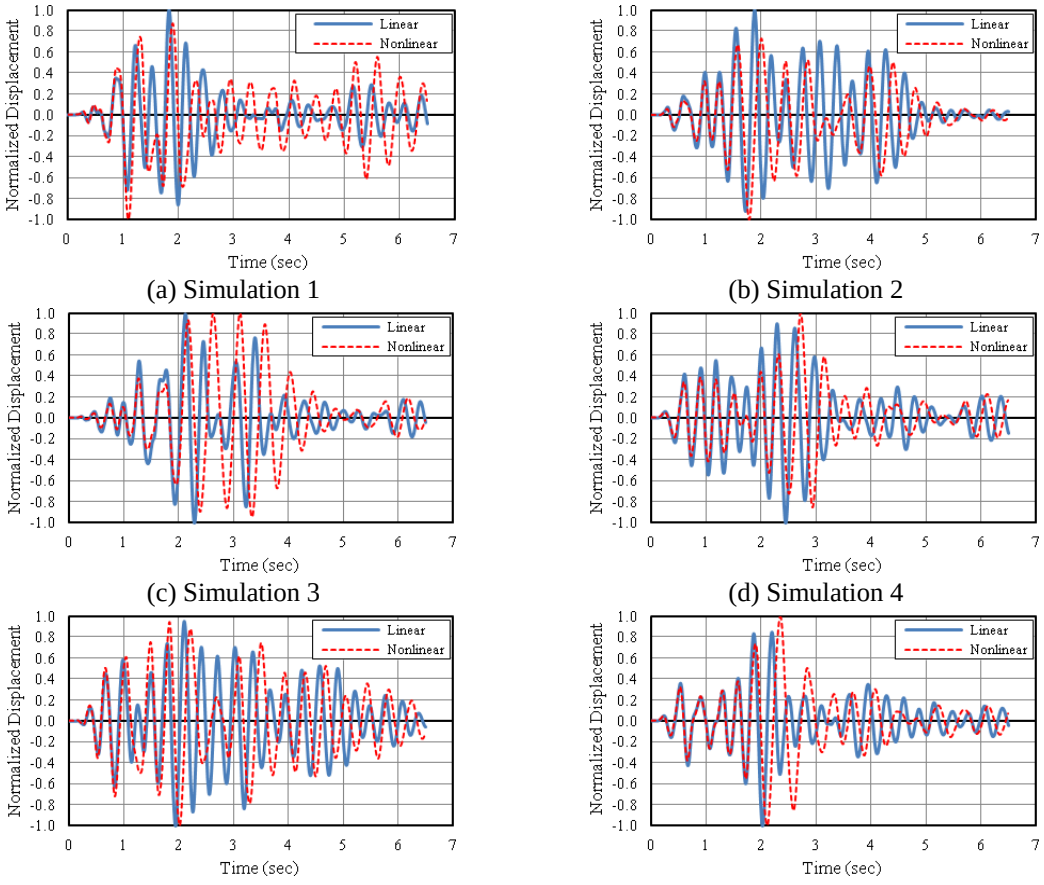

(a) Simulation 1 (b) Simulation 2

(c) Simulation 3 (d) Simulation 4

(e) Simulation 5 (f) Simulation 6

Fig. 8 Normalized response displacement history of SDOF system (for Case 8 of Table 5)

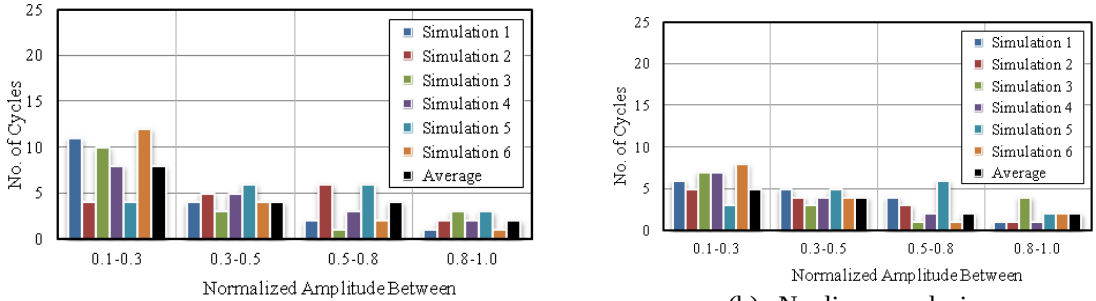

(a) Linear analysis (b) Nonlinear analysis

Fig. 9 Cycle counts for different levels of normalized amplitude (for Case 8 of Table 5)

variabilities. Fig. 10 shows the number of cycles (averaged over all the simulations) for various ranges of normalized amplitude for all the considered cases (i.e. cases 1-12 of Table 5). The following is a list of salient points of observations from these figures

- The number of cycles in a response displacement history tends to decrease with increasing amplitude of normalized displacement for both linear and non-linear responses.
- The number of cycles is slightly less with nonlinear responses as compared to linear responses.
- Results from nonlinear analyses (Fig. 10(b)) show a mean of 9.4 cycles at 0.1-0.3 normalized amplitude, 4.5 cycles at 0.3-0.5 normalized amplitude, 3.3 cycles at 0.5-0.8 normalized amplitude and 2.4 cycles at 0.8-1.0 normalized amplitude.
- The number of cycle decreases as the natural period of the system increases. This reduction is particularly significant at low normalized amplitude.
- Number of cycles increases slightly with increasing magnitude of the earthquake, and particularly so at low normalized amplitude.

The recommended loading protocol derived from the observation (Fig. 10(b)) is shown in Fig. 11 and summarized in Table 6. Despite the large number of cycles observed at low amplitude (0.1-0.3 normalized amplitude), it is recommended to use 4 cycles since the displacement at this phase will be less than the serviceable displacement and would not cause any structural deterioration whether the structure undergoes 4 or 9 displacement cycles. The recommended loading protocol (shown in Fig. 11 and Table 6) uses the displacement control parameter (Δ_M) which refers to the displacement corresponding to 90% of the peak strength at the declining portion of the monotonic load deflection curve (illustrated by Fig. 12). In order to reflect the first onset damage in the structural system, the displacement amplitude at first cycle of the recommended loading history must not exceed the serviceability limit state which can be ensured by limiting the displacement control parameter (Δ_M) as defined by Eq. (2).

Displacement amplitude at 1st cycle < Serviceability displacement limit

$$\begin{aligned} 25\% \text{ of } \Delta_M &< H/300 \\ \Delta_M &< H/75 \end{aligned} \tag{2}$$

where, H is the height of specimen

Serviceability displacement limit = H/300 (Experimental Building Station 1978, Herbert and King 1998)

Monotonic test is required to be performed prior to cyclic test for determining the control displacement parameter (Δ_M). It is expected that the specimen will fail at Δ_M during the cyclic test as the failure displacement in the cyclic test is expected to be less than that in the monotonic test. If the specimen does not fail at Δ_M in the cyclic test, the specimen will be subjected to further tests with larger displacements of three cycles each. Displacement amplitude with increments of 25% of Δ_M will be applied to capture the behavior of the specimen. The test is complete when the recorded resistance drops to 50% of the recorded peak strength (Krawinkler 2009).

It is noted that the recommended loading protocol looks similar (energy dissipating demands are not much different) to the various loading protocols shown in Fig. 1 except for the SPD protocol which consists of large number of high amplitude cycles. However, there is a slight decrease in the total number of displacement cycles in the recommended loading protocol compared to the existing loading protocols. This is due to the fact that the recommended loading

protocol was developed based on low-moderate intensity of ground shaking whereas the other loading protocols shown in Fig. 1 were developed based on stronger intensity of ground shaking.

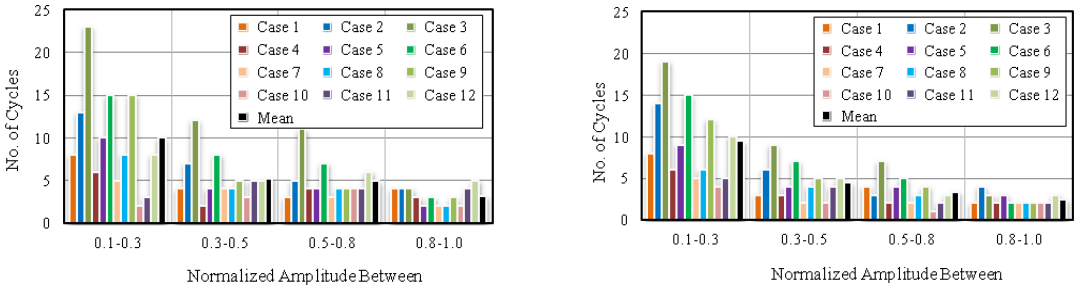

(a) Linear analysis (b) Nonlinear analysis

Fig. 10 Average cycle counts for different levels of normalized amplitude (for all Cases listed in Table 5)

Table 6 Recommended loading protocol

Phase	Number of cycles		Displacement amplitude	
	Observed	Recommended	Observed	Recommended
1	9.4	4	0.1-0.3 of Δ_M	25% of Δ_M
2	4.5	4	0.3-0.5 of Δ_M	50% of Δ_M
3	3.3	3	0.5-0.8 of Δ_M	75% of Δ_M
4	2.4	3	0.8-1.0 of Δ_M	100% of Δ_M
5 - to failure	--	3	--	Increase further by increments of 25% of Δ_M

Table 7 Comparison of number of cycles for 500 and 2500 years RP earthquake scenarios

Displacement amplitude	Observed number of cycles	
	500 Year RP	2500 Year RP
75% of Δ_M	3.3*	5.0**
100% of Δ_M	2.4*	3.7**

* *Refer to* Table 3
** *Refer to* Fig. 13(b)

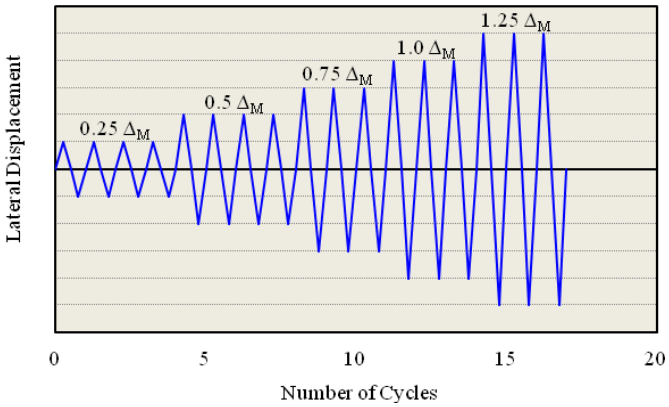

Fig. 11 Recommended loading protocol

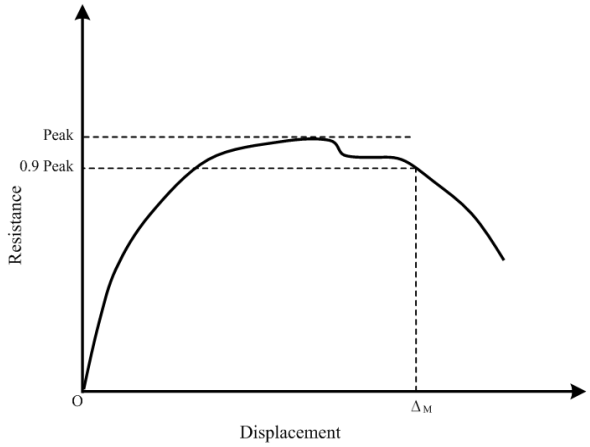

Fig. 12 Determination of displacement control parameter (Δ_M) from monotonic test

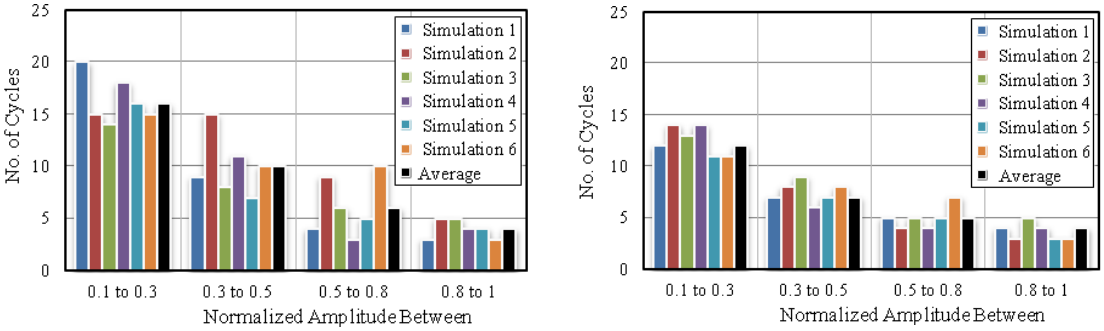

(a) Linear analysis (b) Nonlinear analysis

Fig. 13 Cycle counts for different levels of normalized amplitude for 2500 years RP earthquake Scenario (M = 6.5 & R = 20 km)

A sample simulation has also been performed for the earthquake scenario of M = 6.5 & R = 20 km (k_PZ = 0.21) which is associated with a return period of 2500 years. The number of cycles counted for various levels of normalized amplitude of displacement is shown in Fig. 13. Table 7 presents a comparison of the number of loading cycles obtained for return periods of 500 (Fig. 11) and 2500 (Fig. 13(b)) years. The increased number of displacement cycles with increasing ground motion intensity (from 500 years to 2500 years) is an important observation from the comparative analysis.

6. Conclusions

The main conclusions that can be drawn from this study are as follows:

(a) Earthquake scenarios that are consistent with the current level of hazards stipulated by AS1170.4 (2007) were first identified.

(b) Artificial accelerograms on rock sites have been generated using program GENQKE.

(c) Program SHAKE has been used in order to account for different sub-soil conditions. Response of short-period structure with natural period ranging from 0.1–0.4 sec on site class C is found to be more onerous than on site class D.

(d) Specific earthquake scenarios; such as M = 5.5 & R = 15 km, M = 6.0 & R = 30 km and M = 6.5 & R = 50 km, that affect structure in the natural period range of 0.1–0.4 sec have been identified.

(e) Numerous response time histories (both linear and nonlinear) have been generated for the specific earthquake scenarios and for site class C. Number of cycles is counted between various ranges of normalized amplitude using rain-flow counting method.

(f) Results from nonlinear analyses show a significant decrease in the number of deformation cycles caused by post-elastic behaviour.

(g) A quasi-static cyclic displacement protocol has been developed based on results from nonlinear analyses. The recommended cyclic displacement protocol begins with four cycles at amplitude of 0.25 Δ_M, followed by four cycles at amplitude of 0.5 Δ_M and three cycles each at amplitude of 0.75 Δ_M and 1.0 Δ_M. In order to capture the behaviour of the specimen at larger displacements, the specimen is subject to three cycles each at amplitude with increments of 25% of Δ_M. The test is complete when the resistance drops to 50% of the recorded peak strength.

(h) The recommended loading protocol looks similar to the various existing loading protocols (but with a slightly lower number of displacement cycles compared to the existing loading protocols).

(i) The number of displacement cycles is shown to be dependent on the intensity of ground shaking.

(j) The loading protocol so developed in this paper is intended to guide future experimental work for evaluating design guidelines for lateral bracing elements in domestic buildings built of cold-formed steel.

Acknowledgements

Cash and in-kind support from National Association of Steel-framed Housing (NASH) and financial support from Australian Research Council (ARC) through linkage project (ID LP110100430) entitled “Rational lateral bracing design for steel-framed domestic structures” are acknowledged.

References

AS1170.4 (2007), *Standard Australia*, Structural design actions—Part 4: Earthquake actions in Australia.

ATC-24 (1992), “Guidelines for cyclic seismic testing of components of steel structures for buildings”, *Report No. ATC-24*, Technology Council, Redwood City, CA.

Atkinson, G.M. and Kaka, S.I. (2007), “Relationships between felt intensity and instrumental ground motion in the central United States and California”, *B. Seismol. Soc. Am.*, **97**(2), 497-510.

Atkinson, G.M. and Sonley, E. (2000), “Empirical relationships between modified mercalli intensity and response spectra”, *B. Seismol. Soc. Am.*, **90**(2), 537–544.

Balendra, T., Lam, N.T.K., Wilson, J.L. and Kong, K.H. (2002), “Analysis of long-distance earthquake tremors and base shear demand for buildings in Singapore”, *Eng. Struct.*, **24**(1), 99-108.

Bradley, B.A., Dhakal, R.P., Mander, J.B. and Li, L. (2008), "Experimental multi-level seismic performance assessment of 3D RC frame designed for damage avoidance", *Earthq. Eng. Struct. D.*, **37**(1), 1-20.
Carr, A.J. (2003), *Ruaumoko 2D-Inelastic dynamic analysis*, Department of Civil Engineering, University of Canterbury, Christchurch.
Chandler, A.M. and Lam, N. (2004), "An attenuation model for distant earthquakes", *Earthq. Eng. Struct. D.*, **3**(2), 183-210.
Chandler, A.M., Lam, N. and Tsang, H.H. (2005), "Shear wave velocity modelling in crustal rock for seismic hazard analysis", *J. Soil Dyn. Earthq. Eng.*, **25**, 167-185.
Chandler, A.M., Lam, N. and Tsang, H.H. (2006), "Near surface attenuation modelling based on rock shear-wave velocity profile", *J. Soil Dyn. Earthq. Eng.*, **26**(11), 1004-1014.
Chopra, A.K. (2007), *Dynamics of Structures*, (3rd Ed.), Theory and Application to Earthquake Engineering, Prentice Hall Inc, New Jersey.
Cooney, R.C. and Collins, M.J. (1988), *A wall bracing test and evaluation procedure*, Technical Paper P21, Building Research Association of New Zealand (BRANZ), Judgeford, New Zealand.
Della, C.G., Fiorino, L. and Landolfo, R. (2006), "Seismic behaviour of sheathed cold-formed structures: Numerical study", *J. Struct. Eng., ASCE*, **132**(4), 558-569.
Dhakal, R.P., Mander, J.B. and Mashiko, N. (2006), "Identification of critical ground motions for seismic performance assessment of structures", *Earthq. Eng. Struct. D.*, **35**(8), 989-1008.
Dhakal, R.P., Mander, J.B. and Mashiko, N. (2007), "Bidirectional pseudodynamic tests of bridge piers designed to different standards", *J. Bridge Eng.*, **12**(3), 284-295.
Experimental Building Station (1978), *Guidelines for testing and evaluation of products for cyclone-prone areas*, Technical Record 440, Recommendations of a Workshop Held during July 1977, Department of Construction, James Cook University, Townsville, Australia.
FEMA 461 (2007), *Interim protocols for determining seismic performance characteristics of structural and nonstructural components through laboratory testing*, Prepared by the Applied Technology Council, CA.
Gaull, B.A., Michael-Leiba, M.O. and Rynn, J.M.W. (1990), "Probabilistic earthquake risk maps of Australia", *Australian J. Earth Sciences*, **37**(2), 169-187.
Herbert, P.D. and King, A.B. (1998), "Racking resistance of bracing walls in low-rise buildings subject to earthquake attack", *BRANZ Study Report SR78*, Judgeford, New Zealand.
Hutchinson, G.L., Lam, N.T.K. and Wilson, J.L. (2003), "Determination of earthquake loading and seismic performance in intraplate regions", *Progress Struct. Eng. Mater.*, **5**(3), 181-194.
Idriss, I.M. and Sun J.I. (1992), *User Manual for SHAKE91*, National Institute of Standards and Technology, Maryland, USA and Department of Civil and Environmental Engineering, University of California, Davis, USA.
Iervolino, I. and Cornell, C.A. (2005), "Record selection for nonlinear analysis of structures", *Earthq. Spectra*, **21**(3), 685-713.
King, A.B. and Lim, K.Y.S. (1991), *Supplement to P21: An evaluation method of P21 test results for use with NZS 3604:1990*, Technical Recommendation TR10, Building Research Association of New Zealand (BRANZ), Judgeford, New Zealand.
Krawinkler, H. (1996), "Cyclic loading histories for seismic experimentation on structural components", *Earthq. Spectra*, **12**(1), 1-12.
Krawinkler, H. (2009), "Loading histories for cyclic tests in support of performance assessment of structural components", *Proceedings of the 3rd International Conference on Advances in Experimental Stuctural Engineering*, San Francisco.
Lam, N.T.K. (1999), *Program 'GENQKE' user's Guide*, Department of Civil and Environmental Engineering, The University of Melbourne, Australia.
Lam, N. and Chandler, A. (2005), "Peak displacement demand of small to moderate magnitude earthquakes in stable continental regions", *Earthq. Eng. Struct. Dyn.*, **34**(9),1047-1072.
Lam, N.T.K. and Wilson, J.L. (1999), "Estimation of the site natural period from a borehole record", *Australian J. Struct. Eng.* **1**(3), 179-199.

Lam, N., Asten, M., Roberts, J., Venkatesan, S., Wilson, J., Chandler, A. and Tsang, H.H. (2006), "Generic approach for modelling earthquake hazard", *Invited paper, J. Adv. Struct. Eng.*, **9**(1), 67-82.
Lam, N.T.K., Balendra, T., Wilson, J.L. and Venkatesan, S. (2009), "Seismic load estimates of distant subduction earthquakes affecting Singapore", *Eng. Struct.*, **31**(5), 1230-1240.
Lam, N., Sinadinovski, S., Raymond, K. and Wilson, J. (2003), "Peak ground velocity modelling for Australian intraplate earthquakes", *Int. J. Seismol. Earthq. Eng.*, **5**(2), 11-22.
Lam, N.T.K., Wilson, J.L. and Chandler, A.M. (2001), "Seismic displacement response spectrum estimated from the frame analogy soil amplification model", *Eng. Structures*, **23**(11), 1437-1452.
Lam, N.T.K., Wilson, J.L. and Hutchinson, G.L. (2000), "Generation of synthetic earthquake accelerograms using seismological modelling", *A Review J. Earthq. Eng.*, **4**(3), 321-354.
Lam, N., Wilson, J. and Venkatesan, S. (2005), "Accelerograms for dynamic analysis under the new Australian Standard for earthquake actions", *Electronic J. Struct. Eng.*, **5**, 10-35.
Newmark, N.M. and Rosenblueth, E. (1971), *Fundamentals of Earthuake. Engineering*, Prentice-Hall, New Jersey.
Paton-Cole, V., Gad, E.F., Clifton, C., Heath, D., Davies, C., Hicks, S. and Lam, N.T.K. (2011), "Dynamic performance of a brick veneer house with steel framing", *Australian J. Struct. Eng.*, **11**(3), 231-242.
PEER ground motion database, Beta Version, *http://peer.berkeley.edu/peer_ground_motion_database/*, viewed on 25th September 2011.
Porter, M.L. (1987), "Sequential Phased Displacement (SPD) procedure for TCCMAR testing", *Proceedings of the 3rd Meeting of the Joint Technical Coordinating Committee on Masonry Research*, US-Japan Coordinated Research Program.
Yaghmaei-Sabegh, S. and Lam, N.T.K. (2010), "Ground motion modelling in Tehran based on the stochastic method", *Soil Dyn. Earthq. Eng.*, **30**(7), 525-535.
Yaghmaei-Sabegh, S., Tsang, H.H. and Lam N.T.K. (2011), "Conversion between peak ground motion parameters and modified mercalli intensity values", *J. Earthq. Eng.*, **15**, 1138-1155.

CC